Inorganic Chemistry
Article

Inorg. Chem. **2010**, *49*, 1465–1470 **1465**
DOI: 10.1021/ic901694g

Density Functional Analysis of the Trigonal Uranyl Equatorial Coordination in Hexahomotrioxacalix[3]arene-based Macrocyclic Complexes

Philippe F. Weck,*,† Eunja Kim,‡ Bernardo Masci,§ Pierre Thuéry,¶ and Kenneth R. Czerwinski†

†*Department of Chemistry and Harry Reid Center for Environmental Studies, University of Nevada Las Vegas, 4505 Maryland Parkway, Las Vegas, Nevada 89154,* ‡*Department of Physics and Astronomy, University of Nevada Las Vegas, 4505 Maryland Parkway, Las Vegas, Nevada 89154,* §*Dipartimento di Chimica, Università "La Sapienza", Box 34, Roma 62, P.le Aldo Moro 5, 00185 Roma, Italy, and* ¶*CEA, IRAMIS, SIS2M (CNRS URA 331), LCCEf, Bât. 125, F-91191 Gif-sur-Yvette, France*

Received August 26, 2009

Representative models of the different geometries observed for uranyl complexes with fully deprotonated *p*-R-hexahomotrioxacalix[3]arene (R = *tert*-Bu, Me) ligands, among which is the rare trigonal geometry, have been investigated using all-electron scalar relativistic density functional theory (DFT). Optimized structures of complexes incorporating triethylammonium ($HNEt_3^+$) and 4-methylpiperidinium ($HMePi^+$) cations are in close agreement with experimental crystal diffraction data. Possible explanations for the structural differences between these uranyl complexes are discussed in terms of varying degrees of bonding between uranium and oxygen atoms from the ether and phenoxide groups. In particular, molecular orbital analysis highlights the central role of 5f−2p hybridization in the U−O bonding.

Introduction

The coordination geometry of the uranyl ion $[UO_2]^{2+}$ is strongly constrained by its linear shape, with four to six donor atoms accommodated in the equatorial plane in the vast majority of cases, thus giving the classical polygonal (tetragonal, pentagonal, or hexagonal) bipyramidal uranium environment typical of this ion.[1] However, the last ten years or so have seen the synthesis and structural characterization of several uranyl complexes which represent rare exceptions to this rule. In the case of six-coordination, the equatorial ligands generally define a puckered surface but, when the deviations from the mean plane are sufficiently large, as observed with bulky species such as polypyridines and other polydentate nitrogen-containing ligands, the uranium coordination geometry can best be viewed as rhombohedral or bi(end-capped) trigonal antiprismatic.[2] The unusual seven-coordination in the equatorial plane is achieved when the common chelating nitrato ligand is constrained to be perpendicular to the plane due to steric crowding,[2d,3] which is associated with a slight, but significative departure of the uranyl ion from linearity. Such a slight bending of uranyl is also present with the bulky pentamethylcyclopentadienyl ligand located perpendicular to the equatorial plane.[4] Considering the other end of the coordination number spectrum, the trigonal bipyramidal coordination geometry was first observed in the complex with *p*-*tert*-butylhexahomotrioxacalix[3]arene (or *p*-*tert*-butyl[3.3.3]homooxacalixarene, Scheme 1),[5] a member of the calixarene/oxacalixarene family much investigated for uranyl complexation,[6] and also in a tris[bis(trimethylsilyl)amido] complex.[7] In the first case, the peculiar trigonal geometry arises from the constraints imposed by the macrocyclic ligand displaying three phenoxide groups in a regular array, whereas, in the second case, the amido species is a strong and bulky donor and the coordination sphere is considered to be electronically

*To whom correspondence should be addressed. E-mail: weckp@unlv.nevada.edu.

(1) (a) Katz, J. J.; Seaborg, G. T.; Morss, L. R. *The Chemistry of the Actinide Elements*; Chapman and Hall: London, 1986. (b) Bagnall, K. W. In *Comprehensive Coordination Chemistry*; Wilkinson, G., Gillard, R. D., McCleverty, J. A., Eds.; Pergamon: Oxford, 1987; Vol. *3*, Ch. 40. (c) Wells, A. F. *Structural Inorganic Chemistry*; Clarendon Press: Oxford, 1995.

(2) (a) Berthet, J. C.; Nierlich, M.; Ephritikhine, M. *Chem. Comm.* **2003**, 1660. (b) Berthet, J. C.; Nierlich, M.; Ephritikhine, M. *Dalton Trans.* **2004**, 2814. (c) Sarsfield, M. J.; Helliwell, M.; Raftery, J. *Inorg. Chem.* **2004**, *43*, 3170. (d) Berthet, J. C.; Thuéry, P.; Dognon, J. P.; Guillaneux, D.; Ephritikhine, M. *Inorg. Chem.* **2008**, *47*, 6850.

(3) (a) Charushnikova, I. A.; Den Auwer, C. *Russ. J. Coord. Chem.* **2007**, *33*, 53. (b) Kannan, S.; Moody, M. A.; Barnes, C. L.; Duval, P. B. *Inorg. Chem.* **2008**, *47*, 4691.

(4) Maynadié, J.; Berthet, J. C.; Thuéry, P.; Ephritikhine, M. *Chem. Comm.* **2007**, 486.

(5) Thuéry, P.; Nierlich, M.; Masci, B.; Asfari, Z.; Vicens, J. *J. Chem. Soc., Dalton Trans.* **1999**, 3151.

(6) Thuéry, P.; Nierlich, M.; Harrowfield, J.; Ogden, M. In *Calixarenes*; Asfari, Z., Böhmer, V., Harrowfield, J., Vicens, J., Eds.; Kluwer Academic Publishers: Dordrecht, 2001; Ch. 30, pp 561−582 and references therein.

(7) Burns, C. J.; Clark, D. L.; Donohoe, R. J.; Duval, P. B.; Scott, B. L.; Tait, C. D. *Inorg. Chem.* **2000**, *39*, 5464.

Published on Web 01/07/2010

Scheme 1. *p*-R-hexahomotrioxacalix[3]arene (R = *tert*-Bu **1**, Me **2**)

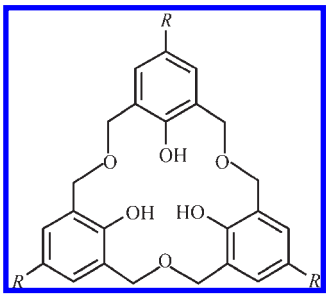

satisfied with only three ligands (although a fourth ligand can be introduced), while the steric saturation is not sufficient to prevent the optional binding of a tetrahydrofuran molecule. Further work with *p*-R-hexahomotrioxacalix[3]arenes (R = Me, *tert*-Bu, C_6H_5, Br), with different bases (mainly amines) added as deprotonating agents, has shown that, upon slight conformational changes of the ether links, one or two ether groups could be involved in weak bonds with uranium, albeit remaining quite distant from the equatorial plane, thus giving much distorted tetragonal or pentagonal bipyramidal coordination environments.[8] Apart from a stereochemical analysis using the method of intersecting spheres,[9] the uranyl trigonal environment has not been investigated from a theoretical viewpoint so far. First-principles approaches are expected to be particularly well suited to shed light on the molecular orbitals involved in the coordination of these uranyl complexes.

Here we report density functional theory (DFT) calculations carried out using representative models of the three different geometries observed with *p*-R-hexahomotrioxacalix[3]arene ligands. Specifically, the structures of the following model uranyl complexes of fully deprotonated *p*-R-hexahomotrioxacalix[3]arene (R = *tert*-Bu **1**, Me **2**), without balancing cation or with incorporation of triethylammonium ($HNEt_3^+$) and 4-methylpiperidinium ($HMePi^+$) cations, have been investigated: $[UO_2(\mathbf{1}-3H)]^-$ (**3**), $[HNEt_3][UO_2(\mathbf{2}-3H)]$ (**4**), and $[HMePi][UO_2(\mathbf{1}-3H)]\cdot 2MeOH\cdot H_2O$ (**5**). The structures of **4** and **5** are compared with available experimental data. Possible explanations for the structural differences between these uranyl complexes are discussed in terms of varying degrees of bonding between uranium and oxygen (ether and phenoxide) atoms.

Details of our computational approach are given in the next section, followed by a discussion and analysis of our results. A summary of our findings and conclusions is given in the last section.

Computational Methods

All-electron scalar relativistic calculations of the total energies, optimized geometries, and molecular properties were performed using density functional theory as implemented in the DMol3 software.[10] The exchange correlation energy was calculated using the local density approximation[11] (LDA) with the parametrization of Perdew and Wang[12] (PWC). The generalized gradient approximation[13] (GGA) employing the PW91 density functional[14] was also tested. GGA functionals such as PW91 or PBE[15] are generally preferred over hybrid functionals which do not appear to describe bonds as accurately in actinide-bearing molecular systems.[16] Double numerical basis sets including polarization functions on all atoms (DNP) were used in the calculations. The DNP basis set corresponds to a double-ζ quality basis set with a *p*-type polarization function added to hydrogen and *d*-type polarization functions added to heavier atoms. The DNP basis set is comparable to 6-31G** Gaussian basis sets[17] with a better accuracy for a similar basis set size.[10] In the generation of the numerical basis sets, a global orbital cutoff of 5.9 Å was used. The energy tolerance in the self-consistent field calculations was set to 10^{-6} Hartree. The molecular geometries of **4** and **5** characterized experimentally by Masci and co-workers[8a] were chosen as initial guesses for the present structural relaxation calculations. Optimized geometries were obtained without symmetry constraints using the direct inversion in a subspace method (DIIS) with an energy convergence tolerance of 10^{-5} Hartree and a gradient convergence of 2×10^{-3} Hartree/Bohr. The charge density was expressed by a nucleus-centered multipole expansion truncated at the octupole level. The spin−orbit coupling was neglected in the calculations as it is expected to be small in a strong ligand-field. This computational approach has shown previously to yield accurate structural results for uranium compounds[18] and various molecular systems.[19]

Results and Discussion

The equilibrium geometries of the uranyl complexes **3**, **4**, and **5** computed using LDA/PWC are represented in Figure 1. The corresponding structural parameters in the environment of the uranium atoms calculated at the LDA/PWC and GGA/PW91 levels of theory are given in Table 1, along with available X-ray diffraction (XRD) data[8a] For **4**, U−O distances and O−U−O angles obtained from the LDA tend to be in better agreement with experiment than GGA results, consistent with previous findings favoring the LDA over the GGA for metal oxide systems.[20] However, both types of functionals reproduce the experimental U−O distances in **5** with a similar accuracy, with a slight advantage to GGA calculations in the description of O−U−O angles. Therefore, for the sake of simplicity, we will focus on LDA results in the rest of the discussion, unless otherwise stated.

The axial uranium-oxo bonds in all three chelates are elongated compared to the U=O distance in the isolated

(8) (a) Masci, B.; Nierlich, M.; Thuéry, P. *New J. Chem.* **2002**, *26*, 120. (b) Masci, B.; Nierlich, M.; Thuéry, P. *New J. Chem.* **2002**, *26*, 766. (c) Masci, B.; Thuéry, P. *Acta Crystallogr., Section E* **2005**, *61*, m2278. (d) Masci, B.; Thuéry, P. *CrystEngComm* **2007**, *9*, 582.
(9) Serezhkin, V. N. In *Structural Chemistry of Inorganic Actinide Compounds*; Krivovichev, S. V., Burns, P. C., Tananaev, I. G., Eds.; Elsevier: Amsterdam, Oxford, 2007; Ch. 2.
(10) Delley, B. *J. Chem. Phys.* **2000**, *113*, 7756.
(11) Kohn, W.; Sham, L. J. *Phys. Rev.* **1965**, *140*, A1133.
(12) Perdew, J. P.; Wang, Y. *Phys. Rev. B* **1992**, *45*, 13244.
(13) Perdew, J. P. *Phys. Rev. B* **1986**, *33*, 8822.
(14) Wang, Y.; Perdew, J. P. *Phys. Rev. B* **1991**, *44*, 13298.
(15) Perdew, J. P.; Burke, J.; Ernzerhof, M. *Phys. Rev. Lett.* **1996**, *77*, 3865.
(16) Shamov, G. A.; Schreckenbach, G.; Martin, R. L.; Hay, P. J. *Inorg. Chem.* **2008**, *47*, 1465.
(17) Hehre, W. J.; Radom, L.; Schleyer, P. R.; Pople, J. A. *Ab Initio Molecular Orbital Theory*; Wiley, New York, 1986.
(18) Weck, P. F.; Kim, E.; Balakrishnan, N.; Poineau, F.; Yeamans, C. B.; Czerwinski, K. R. *Chem. Phys. Lett.* **2007**, *443*, 82.
(19) (a) Weck, P. F.; Dhilip Kumar, T. J.; Kim, E.; Balakrishnan, N. *J. Chem. Phys.* **2007**, *126*, 094703. (b) Kim, E.; Weck, P. F.; Balakrishnan, N.; Bae, C. *J. Phys. Chem. B* **2008**, *112*, 3283. (c) Miller, G.; Kintigh, J.; Kim, E.; Weck, P. F.; Berber, S.; Tomanek, D. *J. Am. Chem. Soc.* **2008**, *130*, 2296. (d) Weck, P. F.; Kim, E.; Poineau, F.; Rodriguez, E.; Sattelberger, A. P.; Czerwinski, K. R. *Inorg. Chem.* **2009**, *48*, 6555.
(20) Wu, Z. G.; Cohen, R. E. *Phys. Rev. B* **2006**, *73*, 235116.

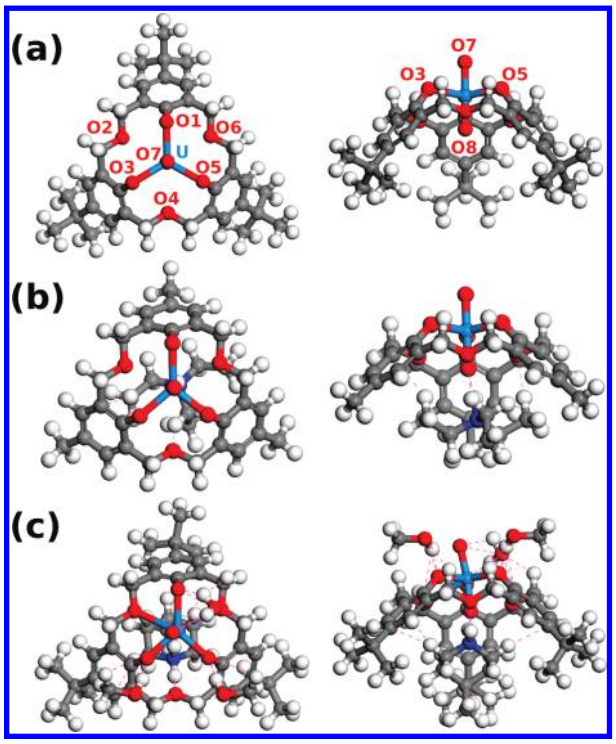

Figure 1. Ball-and-stick representations of the equilibrium structures of the uranyl complexes (a) $[UO_2(\mathbf{1}-3H)]^-$ (**3**), (b) $[HNEt_3][UO_2(\mathbf{2}-3H)]$ (**4**), and (c) $[HMePi][UO_2(\mathbf{1}-3H)]\cdot 2MeOH\cdot H_2O$ (**5**) computed at the LDA/PWC level of theory. Left: top view; right: side view. Color legend: O, red; U, cyan; C, gray; N, navy blue; H, white. Dashed lines in (b) and (c) indicate close contacts.

UO_2^{2+} ion which is predicted to be 1.708 Å with LDA/PWC and 1.724 Å with GGA/PW91, in close agreement with previous fully relativistic results.[21] In addition, the experimental observation of a U−O(7) bond slightly shorter than U−O(8) in **5** is confirmed by calculations. In contrast, the absence of cation and solvent molecules in **3** leads to uranium-oxo bonds nearly identical in length. While oxo ligands are arranged linearly in the complex **3** possessing C_{3v} symmetry, the uranyl unit appears bent toward the O(3) and O(5) atoms of the phenoxide groups in the optimized geometries of **4** and **5**, respectively. Experimental data for the O(7)−U−O(8) bending lie within the ranges of LDA and GGA values, i.e., 179.3−179.6° for **4** and 172.6−177.2° for **5**.

The mean values of the U−O(phenoxide) bond lengths in **4** and **5** structures optimized with LDA (GGA) are 2.207 Å (2.236 Å) and 2.234 Å (2.254 Å), respectively, in close agreement with the experimental values of 2.219(7) Å and 2.238(3) Å. Let us note that the U−O(phenoxide) bond length calculated in **3**, 2.234 Å, is identical to its mean value in **5**, both complexes featuring *p-tert*-butyl substituents. LDA-optimized geometries of **4** and **5** exhibit U−O(1) bonds systematically longer than U−O(3) and U−O(5), similar to the trend apparent in experimental structures.

The U−O(ether) interactions in **3**, **4**, and **5** are rather weak, with bond lengths significantly more elongated than in six-coordinated crown ether uranyl complexes.[22,16] As depicted in Figure 1 for LDA-optimized geometries, only the U−O(2) bond (2.717 Å) is formed in **5** when the upper-limit value of the interatomic distance necessary to create a bond is set to 2.75 Å, i.e., 5% larger than the sum of the covalent radii of O (0.66 Å) and U (1.96 Å) atoms. If the same arbitrary limit of 2.96 Å as in the experimental work of Masci and co-workers[8a] is chosen, ether O(2) and O(6) atoms are predicted to form weak bonds with uranium in both **4** and **5** structures calculated with LDA and GGA whereas, in the crystal structures, only O(2) is considered to be bound in **4** and both O(2) and O(6) in **5**. The mean values of the U−O(2) and U−O(6) bond lengths computed for **4** and **5**, i.e., 2.787 Å and 2.827 Å for LDA and 2.942 Å and 2.853 Å for GGA, respectively, are in fair agreement with the experimental mean values of 2.900 Å and 2.818 Å. Consistent with crystallographic data, the U−O(4) distance is longer than other U−O(ether) bonds by 0.88−0.91 Å in **4** and 1.05−1.26 Å in **5**. These contractions of the U−O(2) and U−O(6) bonds and elongation of U−O(4) compared to the U−O(ether) distance of 3.022 Å (3.155 Å with GGA) in **3** can be seen as antagonistic effects resulting from the introduction of cations in the calixarene cavity of **4** and **5**. The $HNEt_3^+$ and $HMePi^+$ cations are hydrogen-bonded to the oxo group, through the proton bound to nitrogen, with H···O(8) contact distances of 1.478 Å and 1.491 Å (1.596 Å and 1.567 Å with GGA), respectively. The computed distance for **4** appears shorter than the experimental value of 1.92 Å in the crystal sample,[8a] mostly due to the lack of crystal-packing forces pulling the cation out of the calixarene cavity in the present calculations. In **5**, the protons bound to nitrogen were not resolved experimentally, therefore no direct comparison with the calculated H···O(8) distance is possible. Residual distortions arise from the effect of the close contacts of the hydroxy proton of the methanol and water molecules with phenoxide oxygen atoms in **5**, as well as hydrogen bonds formed between the base and the calixarene framework in **4** and **5**.

Partial charges calculated using the Hirshfeld partitioning of the electron density are reported in Table 2 for uranium and oxygen atoms in complexes **3**, **4**, and **5**. Hirshfeld charges are expected to provide a chemically accurate description of the interplay of charge redistribution and structural changes occurring within the complexes upon modification of their molecular environment. The LDA charge carried by U varies from +0.60 *e* for **3** to +0.64−0.65 *e* for **4** and **5**, as more charge is donated from the metal to atoms in its environment. A slight decrease in charge is also observed for oxo and phenoxide oxygens upon addition of cations and solvent molecules. In all three structures calculated with LDA, the charge of the oxo O(8) atom is systematically smaller than the one of oxo O(7) due to its interaction with the neighboring atoms in the calixarene cavity. This contrasts with GGA calculations which suggest that both oxo atoms have identical charge distributions of −0.30 *e* in **4** and −0.29 *e* in **5**. Both LDA and GGA calculations predict the ether O(4) atom to be slightly more negatively charged than its ether O(2) and O(6) congeners engaged in weak bonds with U in **4** and **5**. These findings are further corroborated by cross-sectional views in Figure 2 depicting the electron charge densities in the planes containing the ether O atoms and the phenoxide O atoms. Regions of low charge density appear between the ether oxygen atoms and the uranyl unit in **3**. This contrasts with **4** and **5** where the electron density is essentially continuous between the metal center and the ether O(2) and

(21) de Jong, W. A.; Harrison, R. J.; Nichols, J. A.; Dixon, D. A. *Theor. Chem. Acc.* **2001**, *107*, 22.
(22) Thuéry, P.; Keller, N.; Lance, M.; Vigner, J. D.; Nierlich, M. *New J. Chem.* **1995**, *19*, 619.

Table 1. Selected Interatomic Distances and Angles in the Environment of the Uranium Atom for Complexes **3**, **4**, and **5**

	complex **3**		complex **4**			complex **5**		
parameter[a]	LDA	GGA	LDA	GGA	exp.[b]	LDA	GGA	exp.[b]
				distance (Å)				
U−O(oxo)								
U−O(7)	1.794	1.814	1.789	1.805	1.789(3)	1.803	1.811	1.776(7)
U−O(8)	1.789	1.803	1.843	1.856	1.790(3)	1.824	1.844	1.790(7)
U−O(phenoxide)								
U−O(1)	2.234	2.269	2.225	2.253	2.227(3)	2.257	2.250	2.240(7)
U−O(3)	2.234	2.269	2.193	2.226	2.218(3)	2.222	2.260	2.236(5)
U−O(5)	2.234	2.269	2.203	2.231	2.213(3)	2.223	2.253	2.236(5)
U−O(ether)								
U−O(2)	3.022	3.155	2.771	2.952	2.744(3)	2.717	2.896	2.818(6)
U−O(4)	3.022	3.155	3.685	3.668	3.478(3)	3.982	3.919	3.716(7)
U−O(6)	3.022	3.155	2.804	2.933	3.056(3)	2.937	2.810	2.818(6)
				angle (deg)				
O(7)−U−O(8)	180.0	180.0	179.3	179.6	179.4(1)	172.6	177.2	176.6(3)
O(1)−U−O(2)	65.3	65.0	68.2	67.5	69.1(1)	68.5	67.6	67.0(1)
O(2)−U−O(3)	65.3	65.0	68.5	68.2	69.3(1)	68.8	68.8	69.2(2)
O(1)−U−O(3)	118.9	119.4	129.9	127.1	132.8(1)	134.0	127.8	127.8(1)
O(3)−U−O(5)	118.9	119.4	99.6	103.0	105.8(1)	95.0	98.3	102.4(3)
O(5)−U−O(1)	118.9	119.4	129.5	128.3	120.4(1)	131.0	132.4	127.8(1)

[a] Labeling of the atoms according to the layout in Figure 1. [b] Crystallographic data from Masci, Nierlich, and Thuéry (2002).[8a]

Table 2. Calculated Hirshfeld Atomic Charges (in *e*) of Uranium and Oxygen Atoms for Complexes **3**, **4**, and **5**

	complex **3**		complex **4**		complex **5**	
atom[a]	LDA	GGA	LDA	GGA	LDA	GGA
U	+0.60	+0.67	+0.64	+0.69	+0.65	+0.71
O(oxo)						
O(7)	−0.32	−0.34	−0.29	−0.30	−0.29	−0.29
O(8)	−0.30	−0.30	−0.27	−0.30	−0.25	−0.29
O(phenoxide)						
O(1)	−0.23	−0.24	−0.22	−0.23	−0.20	−0.21
O(3)	−0.23	−0.24	−0.21	−0.22	−0.18	−0.21
O(5)	−0.23	−0.24	−0.21	−0.22	−0.18	−0.21
O(ether)						
O(2)	−0.08	−0.11	−0.08	−0.10	−0.08	−0.10
O(4)	−0.08	−0.11	−0.10	−0.13	−0.09	−0.12
O(6)	−0.08	−0.11	−0.07	−0.10	−0.08	−0.10

[a] Labeling of the atoms according to the layout in Figure 1.

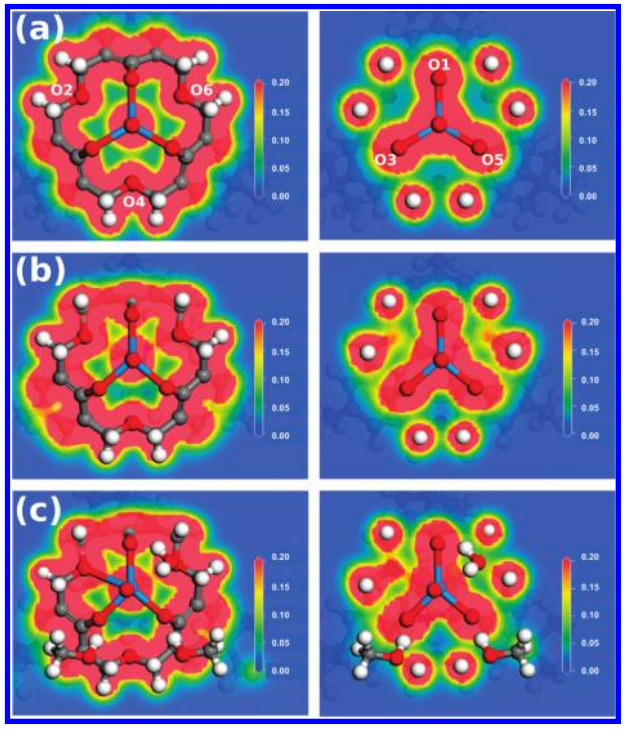

Figure 2. Cross-sectional views of the electron charge densities computed at the LDA/PWC level of theory for the uranyl complexes (a) $[UO_2(\mathbf{1}-3H)]^-$ (**3**), (b) $[HNEt_3][UO_2(\mathbf{2}-3H)]$ (**4**), and (c) $[HMePi][UO_2(\mathbf{1}-3H)]\cdot 2MeOH\cdot H_2O$ (**5**). Slices along the planes containing the ether O atoms (left) and the phenoxide O atoms (right) are represented. Charge densities are plotted in $e/Å^3$ units.

O(6) atoms, while the area between U and O(4) becomes depleted. This explains the shorter bond lengths of U−O(2) and U−O(6) relative to U−O(4). As shown in Figure 2c, a larger degree of asymmetry is observed in the charge density of **5** due to the presence of a solvent water molecule, which accounts for some of the structural distortion observed in this complex. The methanol molecules hydrogen-bonded to the phenoxide groups of the calixarene framework in **5** appear to have only limited effect on the electron density distribution in the environment of the uranium atom.

The molecular orbital (MO) diagram for the model complex **3** with C_{3v} symmetry is shown in Figure 3, along with the major MOs involved in the equatorial U−O bonds. The highest-occupied molecular orbital (HOMO) does not play any role in the U−O bonding. The highest-lying MO responsible for U−O(phenoxide) bonding is the a_1 HOMO − 1, which features three σ bonds along the U−O(phenoxide)

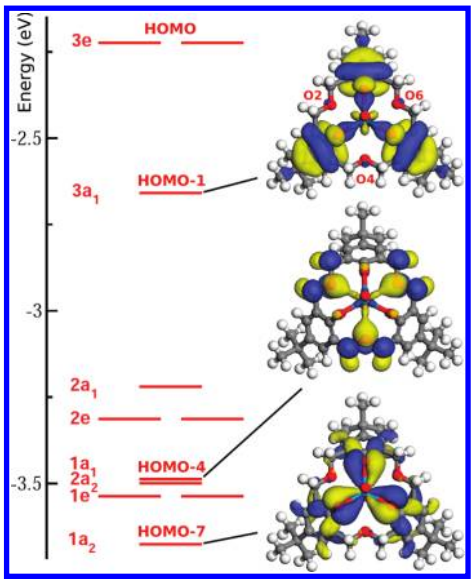

Figure 3. Molecular orbital (MO) energy-level diagram of the complex $[UO_2(\mathbf{1}-3H)]^-$ (**3**) calculated at the LDA/PWC level of theory. Major MOs involved in the uranyl equatorial coordination are represented with an isovalue of 0.02. Labels on the left refer to the Mulliken symbols for the irreducible representations of the group C_{3v} to which the MOs belong. The z direction is chosen along the uranyl axis.

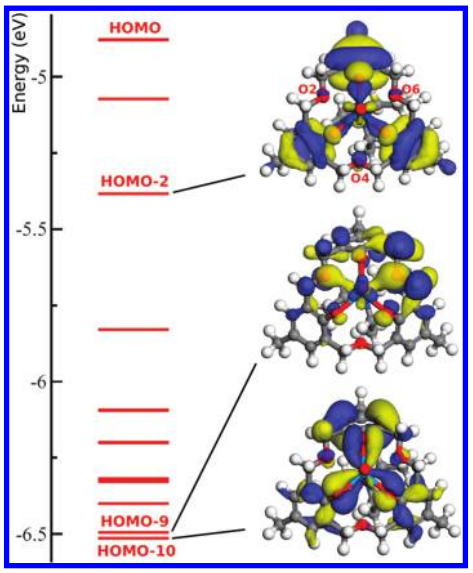

Figure 4. Molecular orbital energy-level diagram of the complex $[HNEt_3][UO_2(\mathbf{2}-3H)]$ (**4**) calculated at the LDA/PWC level of theory. Major MOs involved in the uranyl equatorial coordination are represented with an isovalue of 0.02. The z direction is chosen along the uranyl axis.

directions resulting from constructive overlap of phenoxide O 2p orbitals and the U $5f_{y(3x^2 - y^2)}$ orbital. This 5f orbital possesses six lobes, separated by three nodal planes lying 60° apart which intersect along the z axis of the uranyl unit, and therefore has the proper symmetry to interact with the six neighboring phenoxide and ether oxygen atoms. The $5f_{y(3x^2 - y^2)}$ orbital is also involved in the creation of three weak σ bonds with O(ether) 2p orbitals in the a_1 HOMO − 4. The electron distribution in the σ bonds formed in HOMO − 1 and HOMO − 4 is essentially localized on the oxygen atoms, thus suggesting an ionic character of the U−O bonding. Unlike the $5f_{y(3x^2 - y^2)}$ orbital which forms three σ bonds with oxygen atoms, the $5f_{x(x^2 - 3y^2)}$ orbital mixes with O(phenoxide) 2p orbitals to create π bonds on both sides of the three U−O(phenoxide) directions in a_2 HOMO − 7. The $5f_{x(x^2 - 3y^2)}$ and $5f_{y(3x^2 - y^2)}$ orbitals are related by a 90° rotation about the z−axis passing through the uranyl unit. While the lobes of the $5f_{y(3x^2 - y^2)}$ orbital point directly to phenoxide oxygen atoms, the six lobes of the $5f_{x(x^2 - 3y^2)}$ orbital are oriented 30° apart from their median U−O-(phenoxide) axes, thus sterically promoting π bonding with the lobes of O(phenoxide) 2p orbitals.

The analysis of the MO diagrams of **4** and **5** displayed in Figures 4 and 5, respectively, reveals some U−O bonding characteristics common to all three complexes, such as the preponderant roles of the hybridization of O 2p with U $5f_{y(3x^2 - y^2)}$ and $5f_{x(x^2 - 3y^2)}$ orbitals. Similar to the HOMO − 1 and HOMO − 4 of **3**, the HOMO − 2 and HOMO − 9 of **4** and the HOMO − 4 and HOMO − 10 of **5** are based on the overlap of O 2p and U $5f_{y(3x^2 - y^2)}$ orbitals leading to the formation of U−O σ bonds. The feeble U−O(2) and U−O(6) bonds in **4** and the U−O(2) bond in **5** correspond to the HOMO − 9 and HOMO − 10, respectively. In those two MOs, a noticeable difference with the HOMO − 4 of **3** is the additional mixing of U $5f_{z^3}$. The $5f_{z^3}$ orbital has a planar node in the xy equatorial plane and two conical nodes oriented along the z axis. No evidence of a weak U−O(4) bond was

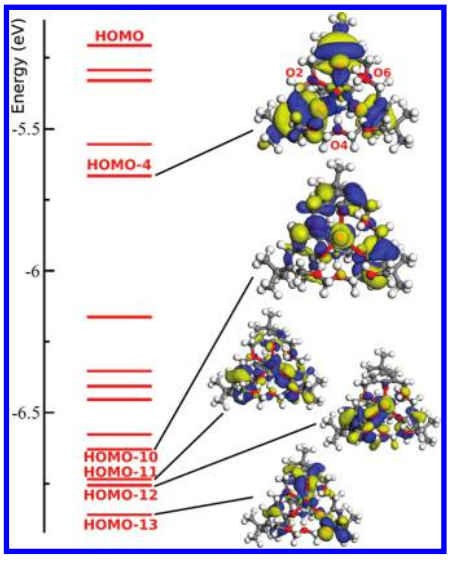

Figure 5. Molecular orbital energy-level diagram of the complex $[HMePi][UO_2(\mathbf{1}-3H)]\cdot 2MeOH\cdot H_2O$ (**5**) calculated at the LDA/PWC level of theory. Major MOs involved in the uranyl equatorial coordination are represented with an isovalue of 0.02. The z direction is chosen along the uranyl axis.

found in the MOs of **4** and **5**, consistent with the elongation of U−O(4) observed in these complexes. While the HOMO − 7 of **3** and the HOMO − 10 of **4** comprise three π bonds resulting from the hybridization of O(phenoxide) 2p and $5f_{x(x^2 - 3y^2)}$ orbitals, the strong structural distortions in **5** lead to a splitting of the corresponding MO energy level into three distinct molecular states, namely the HOMO − 11 (U−O(5) π bond), the HOMO − 12 (U−O(3) π bond), and the HOMO − 13 (U−O(1) π bond). The $5f_{x(x^2 - 3y^2)}$ contribution appears also mixed with some $5f_{z^3}$ component in these three MOs.

A standard indicator of kinetic stability and chemical hardness of molecular systems is given by the energy separation between the highest occupied molecular orbital

(HOMO) and the lowest unoccupied molecular orbital (LUMO), a large energy gap implying high stability.[23,24] The energy gap between frontier MO levels calculated at the LDA/PWC level of theory is 2.18 eV for **3**, significantly larger than the values of 1.67 eV for **4** and 1.60 eV for **5**. These results suggest that the introduction of cations in the calixarene cavity and the addition of solvent molecules tend to slightly decrease the overall stability of these isolated uranyl complexes.

Conclusion

All-electron scalar relativistic calculations have been carried out within the framework of density functional theory to investigate metal−ligand bonding in representative models of uranyl coordination complexes with fully deprotonated *p*-R-hexahomotrioxacalix[3]arene (R = *tert*-Bu, Me) ligands. Optimized structures of complexes incorporating the triethylammonium ($HNEt_3^+$) and 4-methylpiperidinium ($HMePi^+$) cations are in overall good agreement with experimental crystal diffraction data. U−O(phenoxide) bonds are formed and U−O(ether) interactions in the complexes remain relatively weak. Upon introduction of ammonium ions in the calixarene cavity of these uranyl complexes, a contraction of two of the U−O(ether) bonds occurs, while the remaining U−O(ether) bond tends to be elongated. Molecular orbital analysis highlights the central role of 5f−2p hybridization in the U−O bonding. In particular, the U $5f_{y(3x^2 - y^2)}$ orbital overlaps constructively with 2p orbitals of phenoxide and ether oxygen atoms to form U−O σ bonds. In addition, the hybridization of O(phenoxide) 2p and $5f_{x(x^2 - 3y^2)}$ orbitals leads to the creation of U−O(phenoxide) π bonds. Molecular orbital calculations also suggest that the presence of cations in the calixarene cavity and the addition of solvent molecules slightly decreases the overall kinetic stability and chemical hardness of these isolated uranyl complexes.

All-electron relativistic DFT investigation of inclusion complexes formed between similar deprotonated *p*-R-hexahomotrioxacalix[3]arene ligands and other actinyl ions (e.g., $[AnO_2]^{n+}$, $n = 1$ and 2, An = Np and Pu) should provide further insight into the interplay of steric and electronic factors governing metal−ligand coordination in this class of complexes.

Acknowledgment. Funding for this research was provided by the U.S. Department of Energy, Cooperative Agreement DE-FG07-01AL6735B.

(23) Manolopoulos, D. E.; May, J. C.; Down, S. E. *Chem. Phys. Lett.* **1991**, *181*, 105.
(24) Pearson, R. G. *Hard and Soft Acids and Bases*; Dowden, Hutchinson and Ross: Stroudsburg, PA, 1973.